Physics and Astronomy   College of Arts and Sciences

1996

Type-II Interface Exciton in ZnSe/(Zn,Mn)Se Heterostructures

V V. Rossin

Thomas Böttger
University of San Francisco, tbottger@usfca.edu

F Henneberger

Follow this and additional works at: http://repository.usfca.edu/phys

Part of the Physics Commons

Recommended Citation

Rossin, V.V., Böttger, T., Henneberger, F. Type-II interface exciton in ZnSe/(Zn,Mn)Se heterostructures (1996) Physical Review B - Condensed Matter and Materials Physics, 54 (11), pp. 7682-7685. https://doi.org/10.1103/PhysRevB.54.7682

Type-II interface exciton in ZnSe/(Zn,Mn)Se heterostructures

V. V. Rossin

A. F. Ioffe Physico-Technical Institute, St. Petersburg 194021, Russia

T. Böttger and F. Henneberger

Humboldt-Universität zu Berlin, Institut für Physik, Berlin 10115, Germany

(Received 2 May 1996)

Two emission bands are observed in the photoluminescence spectrum of ZnSe/(Zn,Mn)Se heterostructures. These bands emerge in a magnetic field and are associated with interface excitons formed as a result of a magnetic-field-induced type-I–type-II transition of the band alignment. Time-resolved measurements yield lifetimes in the ns range signifying a relatively large spatial separation of electrons and holes and hence low optical oscillator strength. These features are confirmed by a theoretical analysis of the interface exciton state revealing a reduced importance of the electron-hole Coulomb interaction in comparison with type-II excitons in quantum wells. [S0163-1829(96)03435-2]

In semidilute or dilute magnetic semiconductors (DMS's), the Zeeman splitting of the carrier states is greatly enhanced due to the s, p-d exchange interaction with localized magnetic ion moments.[1] The use of these materials in heterostructures (e.g., in combination with nonmagnetic layers) offers the unique possibility to tailor the band offsets spin selectively by an external magnetic field. One of the related phenomena is the formation of spin superlattices.[2–4] For prototype II-VI DMS's, the hole exchange coupling is typically a factor 4–5 stronger than for electrons. Therefore, choosing a zero-field valence-band offset that is small enough, a magnetic-field-induced type-I – type-II transition of the band alignment can be accomplished.[5–9] (Zn, Mn)Se/ZnSe is a system where this transition is easily observed at relatively low magnetic fields ($B \approx 2$ T).[7–9] In the situation of type-II alignment, the spatial separation of the electron and hole, confined now in different layers, will reduce the oscillator strength for the optical transition.[10] However, the Coulomb interaction can partly compensate for this tendency, and establish an indirect or type-II exciton state where the electron and hole are still significantly correlated. Indeed, studies on (Zn,Mn)Se/ZnSe quantum-well (QW) excitons have not revealed any dramatic change of the optical absorption and lifetime.[7–9] On the other hand, the existence of a long-lived type-II exciton magnetic polaron was recently claimed for ZnSe/(Zn,Mn)Se superlattice structures.[11] In this paper, we report on the direct observation of an emission from a single heterointerface exciton formed above a critical field by electrons and holes situated in different (bulklike) layers. The design of the DMS structures used in our study allowed us to monitor simultaneously the magnetic-field behavior of a DMS QW exciton, and to figure out the qualitatively different role of the Coulomb interaction in these two excitonic states.

The samples were fabricated by molecular-beam epitaxy on GaAs substrate on which, first, a 1-μm-thick ZnSe bulk layer (BL) was grown. This layer is followed by a 35-nm-wide $Zn_{0.8}Mn_{0.2}Se$ barrier and a ZnSe QW of a width close to the ZnSe exciton Bohr radius ($\alpha_B = 4.5$ nm). The structure is completed by a $Zn_{0.8}Mn_{0.2}Se$ cap layer again 35 nm thick.

The samples were mounted in the bore of superconducting split-coil magnet capable of fields up to 12 T. The circularly polarized cw photoluminescence (PL) and PL excitation (PLE) spectra were studied at temperatures from 1.6 to 10 K using a tunable dye laser (Stilbene 3) pumped by an argon-ion laser. For time-resolved measurements, a synchronously pumped tunable dye laser with a pulse duration of 2 ps and 76-MHz repetition rate was used. The PL was recorded either with a synchroscan streak-camera (time resolution 5 ps) or a time-correlated single-photon counting system of better dynamic range but worse time resolution (50 ps).

PL data at $T = 1.6$ K are summarized for different magnetic fields in Fig. 1(a). The PL spectrum at zero field exhibits a line from the QW heavy-hole exciton (X_{hh}) and emission from the ZnSe BL. Unlike previously studied multiple QW structures of similar design but thicker barriers[8,9] [where the QW is under tensile strain, the ground-state exciton of light-hole nature (X_{lh}) and shifted below the ZnSe bulk resonance], the barriers are compressively strained by the much thicker ZnSe BL in the present samples. Since the position of the QW excitons is now dominated by confinement effects, X_{hh} is the one of lowest energy and appears on the high-energy side of the ZnSe emission. This assignment is directly confirmed by the magnetic-field dependencies of the resonances seen in PLE (Fig. 2). The Zeeman splitting of X_{hh} is much larger than for X_{lh} located 11 meV above X_{hh} at $B = 0$ T. The emission from the ZnSe BL consists of a free-exciton line on the high-energy side, and bound-exciton features with a dominant I_2 peak at 2.7945 eV. When a magnetic field in Faraday geometry is applied, the X_{hh} line in PL undergoes a pronounced low-energy shift while the emission from the nonmagnetic ZnSe BL stays at fixed energies. At a magnetic field $B > 0.5$ T, an additional line (H_1) appears in PL energetically below the ZnSe bound exciton. The PLE spectrum of H_1 [Fig. 1(b)] displays the exciton of both the ZnSe BL and (Zn,Mn)Se barrier, but no indication of the resonance itself (under detection at the low-energy side of the H_1 PL band) is seen. Contrary to the emission from ZnSe, the H_1 feature is strongly circularly polarized (σ^+) and exhibits a distinct low-energy shift with increasing mag-
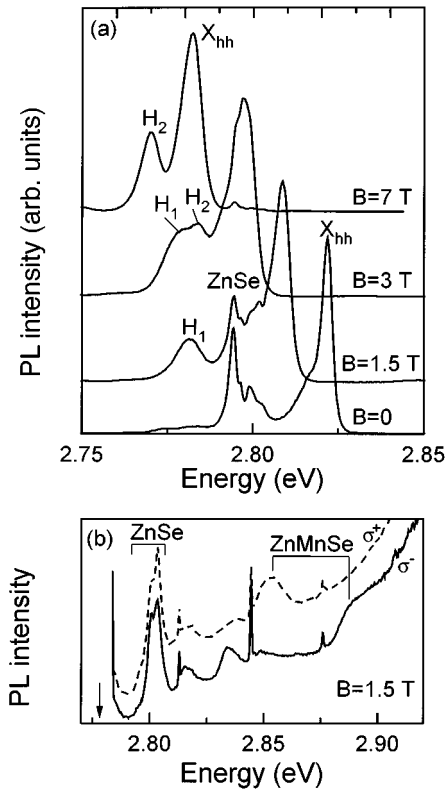
FIG. 1. PL spectra in σ^+ polarization at various magnetic fields (a) and PLE spectra detected at H_1 for $B = 1.5$ T (b).

netic field, being, however, somewhat smaller than for X_{hh} (Fig. 2). At $B = 3$ T, a second line (H_2) emerges 4 meV above the H_1 position. Under further field increase, H_1 disappears and H_2 becomes the only PL feature on the low-energy side of X_{hh}. As is seen from Fig. 2, H_2 shifts practically parallel to X_{hh} with B. The PLE spectrum of H_2 is similar to the one of H_1, with resonances from the ZnSe BL and (Zn,Mn)Se barrier. The different nature of H_1 and H_2, however, is documented by the fact that the former line dis-
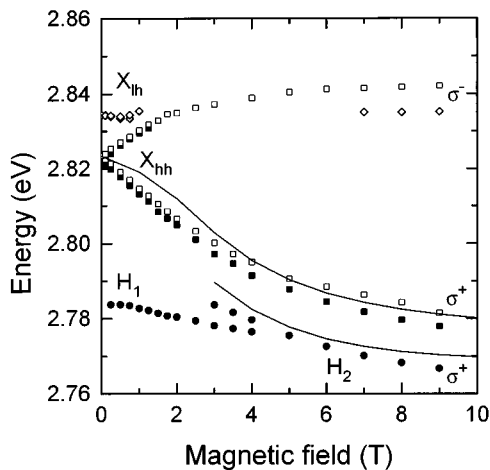

FIG. 2. Energy positions of PLE (open symbols) and PL (filled symbols) peaks vs magnetic field. The solid lines represent the calculated magnetic-field dependencies of QW and heterointerface exciton energies.
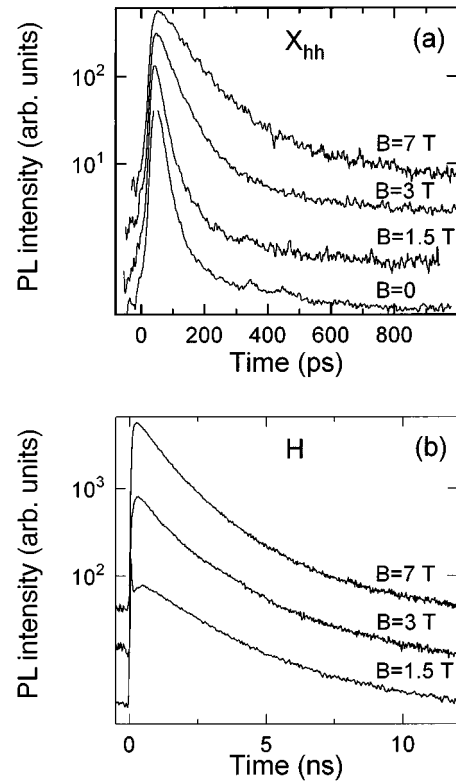

FIG. 3. PL decay kinetics for different magnetic fields measured at the X_{hh} peak (a), H_1 peak [(b), $B = 1.5$ T], H_2 peak [(b), $B = 3.0$ and 7.0 T). Traces are arbitrarily shifted along the y axis.

appears at slightly larger temperatures (10 K), whereas the appearance of H_2 is merely shifted to somewhat higher fields.

Time-resolved measurements demonstrate that the kinetics of both H lines is quite similar but totally different from that of X_{hh} and the ZnSe BL exciton. Figure 3(a) shows the time behavior of the X_{hh} line for various magnetic fields. At $B = 0$, when X_{hh} is the energetically highest feature in the PL spectrum, its decay is very fast, with a time constant of 13 ps extracted by deconvolution of the experimental decay transients with the apparatus function. In a magnetic field, this time increases continuously, reaching a value of 107 ps at $B = 9$ T. In marked contrast, the decay of the H lines depicted in Fig. 3(b) evolves on the ns time scale, and the 1/e lifetime decreases from 2.2 ns and $B = 1.5$ T (H_1) to 1.1 ns at $B = 7$ T (H_2).

The experimental data allow us to conclude that the H lines represent emission from the heterointerface between the ZnSe BL and the (Zn,Mn)Se barrier. Direct evidence of this is that both lines are effectively excited via absorption at both sides of this interface. The field range of their emergence is close to the one observed previously for the type-I–type-II transition on multiple-QW structures of similar Mn concentrations.[8,9] Thus an electron situated in the ZnSe BL recombines with a hole in the (Zn,Mn)Se barrier, explaining the long lifetimes and why no indication of the H features is found in PLE. However, though separation of electron and hole also occurs for the QW exciton, its behavior is strikingly different. This is a consequence of the much stronger role of the Coulomb interaction. To confirm this quantita-

tively, we have numerically solved the Schrödinger equation for both the QW and interface exciton. The Hamiltonians for the along-growth-axis (z) and in plane [two-dimensional (2D)] motion read as

$$H^z = \sum_{i=e,h} \left\{ -\frac{\hbar^2}{2m_i} \frac{\partial^2}{\partial z_i^2} + V_i(z_i, B) \right\}, \qquad (1)$$

$$H^{2D} = -\frac{\hbar^2}{2\mu} \frac{1}{\rho} \frac{\partial}{\partial \rho} \rho \frac{\partial}{\partial \rho} - \frac{e^2}{\varepsilon \sqrt{\rho^2 + z^2}} + \frac{e^2 B^2}{8\mu} \rho^2 \qquad (2)$$

[$z_{e/h}$ and $m_{e/h}$ are the electron (hole) position and effective mass in the growth direction, respectively, $z = z_e - z_h$, ρ is the electron-hole relative in-plane coordinate, μ is the reduced in-plain mass, and ε is the dielectric constant]. The external magnetic field ($\mathbf{B} \| z$) enters both parts, but the major role is played by the field-dependent band offsets

$$V_i(z_i, B) = \theta(z_i) \left\{ \Delta V_i - 1/2 x S_0 \alpha_i B_{5/2} \left[\frac{g\mu_B B}{k_B(T+T_0)} \right] \right\}, \qquad (3)$$

with $\theta(z)$ as the Heaviside function defining the interface at $z = 0$, and ΔV_i ($i = $e and h) as the zero-field potential barriers. When the QW exciton is considered, $\theta(z)$ is replaced by $\theta(-z)\theta(z-d)$, with d as the well width. The magnetization of the Mn^{2+} ions in mean-field approximation is expressed by the Brillouin function $B_{5/2}$ with the Mn^{2+} g factor, x is the Mn concentration, and the α_i's are the exchange constants. The phenomenologically introduced quantities T_0 and S_0 account for antiferromagnetic pairing of the Mn^{2+} spins.[12] Following Refs. 13 and 14, we look for a solution of the form $\Psi(\mathbf{r}_e, \mathbf{r}_h) = \Phi(z_e, z_h) g_1(\rho, z)$, where g_1 is the ground state of

$$H^{2D} g_1(\rho, z) = E_1^{2D}(z) g_1(\rho, z). \qquad (4)$$

The function Φ obeys the equation

$$[H^z + E_1^{2D}(z) + W_1(z)] \Phi(z_e, z_h) = E\Phi(z_e, z_h), \qquad (5)$$

with

$$W_1(z) = \frac{\hbar^2}{2\mu_z} \int_0^\infty \left| \frac{\partial g_1(\rho, z)}{\partial z} \right|^2 \rho \, d\rho$$

comprising the kinetic energy associated with the relative motion of the particles along the growth axis ($1/\mu_z = 1/m_e + 1/m_h$). E_1^{2D} is obtained by straightforward numerical solution of (4). The function $W_1(z)$ is substituted by $\delta W_1(z) = W_1(z) - \lim_{n\to\infty} W_n(z)$, an analytical fit of which is given in Ref. 14. Equation (5) is solved by the method of successive iterations,[10] factoring the function $\Phi(z_e, z_h) = \phi(z_e)\phi(z_h)$ and tackling the respective single-particle equations obtained by integration over the other coordinate. We start with an arbitrary Gaussian for $\phi(z_e)$ and continue until the procedure converges. The parameter set used in the calculations $m_e = 0.15 m_0$, $m_{hh} = 0.8 m_0$, $\varepsilon = 8.8$ (Ref. 15), $\mu = 0.1 m_0$ (Ref. 16), $\alpha_e = 0.26$ eV and $\alpha_h = 1.31$ eV (Ref. 12), and $S_0 = 0.53$ and $T_0 = 4.4$ K (Ref. 9). The band offsets were adjusted to reproduce the Zeeman shifts of X_{hh} and H_2 observed experimentally (see Fig. 2). Their values ($\Delta V_e = 50$ meV and $\Delta V_{hh} = 15$ meV) are in the range of
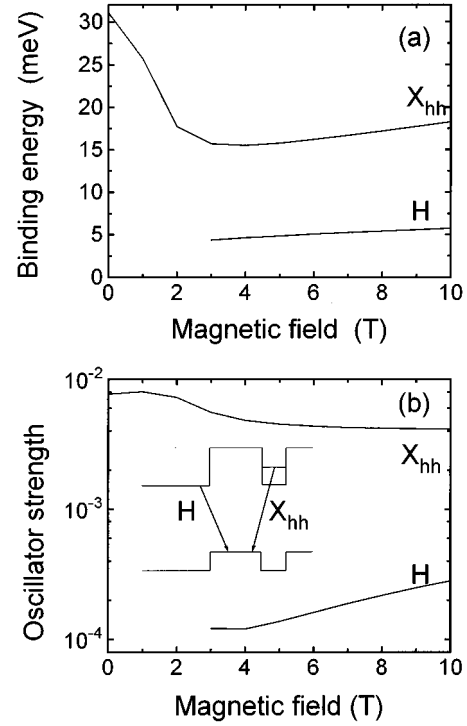

FIG. 4. Calculated binding energy (a) and oscillator strength (b) for QW and heterointerface excitons (shown schematically in the inset), respectively, vs magnetic field.

previously published data,[9,17] and yield the type-I–type-II transition for $B = 0.85$ T. In the calculations, the interface exciton becomes stable at a somewhat larger B when the absolute value of the valence-band offset exceeds the difference of bulk and interface exciton binding energies.

Figure 4 presents the binding energy, calculated relative to the transition between the zeroth-order Landau levels following from (4) when the Coulomb interaction is omitted, and the oscillator strength of both exciton species. In the QW exciton, the electron is held close to the interface ($\approx d/2 = 2.25$ nm) through the confinement and, in combination with the Coulomb interaction, a significant electron-hole overlap is hence maintained. Conversely, for a single heterointerface, the maximum of the electron probability occurs at much farther distance ($\approx 1.5\alpha_B = 6.8$ nm) decreasing the role of Coulomb effects. The binding energy of the interface exciton amounts only about 1/3 of the one in QW geometry and its oscillator strength is even more than one order of magnitude smaller. These results confirm strikingly the above conjecture about the different internal structure of QW and interface exciton. The slight increase of the binding energy seen for both excitons at larger fields in Fig. 4(a) is related to a shrinkage of the in-plane radius caused by the B^2-term in H^{2D}. For H, this increase is reinforced by a shift of the electron towards the heterointerface caused by the decreasing conduction band offset. The related rise of the oscillator strength is in fact experimentally indicated for the interface excitons by the tendency of longer lifetimes in Fig. 3(b).

Though our experimental results demonstrate unambiguously that both H features are related with the heterointerface, it is obvious that only H_2 can be identified with the ''intrinsic'' interface state treated theoretically above. The

origin of H_1 needs further investigation. One of our current hypotheses is localization on magnetic fluctuations since the line is rapidly quenched by an external field or lattice heating. The long lifetimes of the H lines are of radiative origin. Conversely, the fast decay of X_{hh} at $B=0$ is caused by non-radiative processes. One possible explanation is energy transfer via barrier states that are energetically close to the QW excitons for the present structure design. In fact, we observe a relatively bright 2.1 eV emission on these samples. That situation is qualitatively different from dilatation strained QW's where the groundstate (X_{lh}) is distinctly low-energy shifted with respect to bulk ZnSe. The fast non-radiative exciton decay prevents the formation of an exciton magnetic polaron observed previously under tensile strain conditions.[8,9] At higher magnetic fields, the 2.1 eV Mn emission becomes increasingly quenched and the longer PL decay lifetimes are now consistent with data reported previously for radiative recombination.[9,18]

In conclusion, we have demonstrated the formation of a heterointerface exciton due to a magnetic-field-induced type-I–type-II transition in ZnSe/(Zn,Mn)Se heterostructures. Its appearance (small binding energy, low oscillator strength, long lifetime) is clearly distinguished from a type-II QW exciton studied on the same heterostructure for which the electron-hole Coulomb interaction is still the dominating factor.

[1] J.K. Furdyna, J. Appl. Phys. **64**, R29 (1988).

[2] M. von Ortenberg, Phys. Rev. Lett. **49**, 1041 (1982).

[3] W. C. Chou, A. Petrou, J. Warnock, and B. T. Jonker, Phys. Rev. Lett. **67**, 3820 (1991).

[4] N. Dai, H. Luo, F. C. Zhang, N. Samarth, M. Dobrowolska, and J. K. Furdyna, Phys. Rev. Lett. **67**, 3824 (1991).

[5] X. Liu, A. Petrou, J. Warnock, B. T. Jonker, G. A. Prinz, and J. J. Krebs, Phys. Rev. Lett. **63**, 2280 (1989).

[6] E. Deleporte, J. M. Berroir, G. Bastard, C. Delalande, J. M. Hong, and L. L. Chang, Phys. Rev. B **42**, 5891 (1990).

[7] E. Deleporte, T. Lebihen, B. Ohnesorge, Ph. Rossignol, C. Delalande, S. Guha, and H. Munekata, Phys. Rev. B **50**, 4514 (1994).

[8] V. V. Rossin, J. Puls, and F. Henneberger, Phys. Rev. B **51**, 11 209 (1995).

[9] V. V. Rossin, F. Henneberger, and J. Puls, Phys. Rev. B **53**, 16 444 (1996).

[10] J. Warnock, B. T. Jonker, A. Petrou, W. C. Chou, and X. Liu, Phys. Rev. B **48**, 17 321 (1993).

[11] C. G. Poweleit, L. M. Smith, and B. T. Jonker, Phys. Rev. B **50**, 18 662 (1994).

[12] A. Twardowski, M. von Ortenberg, M. Demianiuk, and R. Panthenet, Solid State Commun. **51**, 849 (1984).

[13] R. P. Leavitt and J. W. Little, Phys. Rev. B **42**, 11 774 (1990).

[14] P. Peyla, R. Romestain, Y. Merle d'Aubigne, G. Fishman, A. Wasiela, and H. Mariette, Phys. Rev. B **52**, 12 026 (1995).

[15] *Intrinsic Properties of Group IV Elements and III-V, II-VI, and I-VII Compounds*, edited by O. Madelung and M. Schulz, Landolt-Börnstein, New Series, Group IV, Vol. 22, Pt. a (Springer, Berlin, 1987).

[16] J. Puls, V. V. Rossin, F. Heneberger, and R. Zimmermann, Phys. Rev. B **54**, 4974 (1996).

[17] Streller, N. Hoffman, A. Schülzgen, J. Griesche, H. Babucke, F. Henneberger, and K. Jacobs, Semicond. Sci. Technol. **10**, 201 (1995).

[18] A. Schülzgen, F. Kreller, F. Henneberger, M. Lowisch, and J. Puls, J. Cryst. Growth **138**, 575 (1994).